Aptamer Conformation-Cooperated Enzyme-Assisted Surface-Enhanced Raman Scattering Enabling Ultrasensitive Detection of Cell Surface Protein Biomarkers in Blood Samples

Yingying Li,[†] Qianqian Fang,[†] Xinxing Miao,[†] Xiuyan Zhang,[‡] Yun Zhao,[‡] Jun Yan,[†] Yiqiu Zhang,[†] Renfei Wu,[†] Baoqing Nie,[§] Michael Hirtz,[∥] and Jian Liu*[,†]

[†]Institute of Functional Nano and Soft Materials (FUNSOM), Jiangsu Key Laboratory for Carbon Based Functional Materials and Devices, Joint International Research Laboratory of Carbon Based Functional Materials and Devices, and [‡]Cyrus Tang Haematology Centre, Jiangsu Institute of Haematology, The First Affiliated Hospital, Soochow University, Suzhou, Jiangsu Province 215123, China

[§]School of Electronic and Information Engineering, Soochow University, Suzhou, Jiangsu Province 215006, China

[∥]Institute of Nanotechnology (INT) and Karlsruhe Nano Micro Facility (KNMF), Karlsruhe Institute of Technology (KIT), Karlsruhe 76131, Germany

ABSTRACT: Developing novel strategies for sensitive and specific detection of protein biomarkers is a field of active research. Here, we report an ultrasensitive biosensor to detect protein tyrosine kinase 7 (PTK7), an important protein biomarker on the cell surface, by aptamer conformation cooperated enzyme assisted surface enhanced Raman scatter ing (SERS) (ACCESS) technology. Our approach features a synergistic combination of the conformational alteration of the anglerfish aptamer triggered by the recognition of the membrane protein (PTK7) and Exo III enzyme assisted nucleic acid amplification. It transduces the specific binding events between the aptamer and PTK7 protein into dramatically improved SERS signals. Sensitive and specific detection of PTK7 protein has been demonstrated both in the solution and directly on the surface of live CCRF CEM cells, with a limit of detection better than the commercial enzyme linked immunosorbent assay method by nearly 5 orders of magnitude. As a flexible, ultrasensitive, and specific approach, ACCESS promises important applications in clinical diagnostics, where only a very limited amount of the biological sample is available.

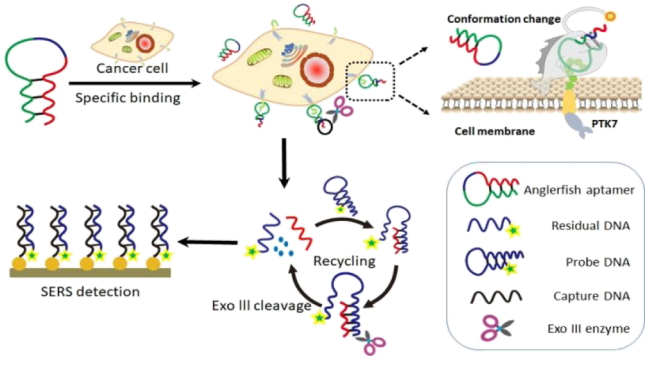

KEYWORDS: *DNA nanotechnology, aptamer, SERS, signal amplification, protein biomarker*

Mutations or aberrant expression of membrane proteins have been associated with numerous human dis eases.[1−5] Protein tyrosine kinase 7 (PTK7), also known as colon carcinoma kinase 4 (CCK 4), is a membrane receptor encoded by the PTK 7 gene.[6−8] PTK7 plays an important role in modulating multiple Wnt pathways.[9−11] Accumulated evidence suggests that PTK7 is overexpressed in various tumors such as T cell acute lymphoblastic leukemia (T ALL), acute myeloid leukemia (AML), colon cancer, gastric cancer, and lung cancer.[12−16] Researchers have been utilizing several representative assays for the detection of PTK 7 protein, such as western blotting, flow cytometry, and enzyme linked immunosorbent assay (ELISA).[17−20] Although western blot ting is a classical tool in cell signaling studies, it demands a step of cell lysis, thus losing the information of cell integrity/viability. It can only provide semiquantitative results in protein detection. Flow cytometry is a high throughput technique, but it requires a large number (10^5 to 10^6) of cell samples for statistically meaningful segmentation of the cell subpopula tions.[17,21] ELISA is a widely used immunoassay which typically involves horseradish peroxidase (HRP) enzyme activity for signal amplification. This technique suffers from several limitations such as uncertainty of multiple epitopes or the risks of false positive results by the cross reactivity in antigen−antibody recognition.[22,23] Aptamers are single stranded oligonucleotide sequences screened for high binding affinity and selectivity for specific analytes, being analogous to "chemically synthesized antibodies".[24−28] The aptamer se quence (sgc8) specific to PTK 7 protein has been proposed to be hybridized to a G quadruplex forming sequence, allowing for fast and sensitive signal on detection of this protein

biomarker using a luminescent iridium(III) complex.[29] A metal−organic framework enhanced aptasensor has further been developed for electrochemical detection of PTK7 with the range of pg mL^{-1}as the limit of detection (LOD).[30] However, those methods still demand the lysis steps to collect cell debris for protein detection. There remains a great need to develop novel strategies for sensitive and specific detection of PTK7 biomarkers directly on the surface of live cells, especially for the applications requesting cell recovery to perform subsequent tests on cell proliferation, migration, or drug screening.

In our previous work, we developed a useful tool for ultrasensitive signal on detection of genetic biomarkers (LOD ≈ 1 aM) by integrating exonuclease III assisted DNA amplification and surface enhanced Raman scattering (SERS).[31] But there was still a question left unattended whether other types of biomolecular targets besides nucleic acids can be detected by this new technology. Here, we report an important concept to address this question, and demonstrate that protein biomarkers on live cell membranes can be sensitively detected by aptamer conformation cooperated enzyme assisted SERS (ACCESS) technology. The biosensor features a combination of aptamer conformation alteration triggered by the recognition of the membrane protein (PTK7) and Exo III enzyme assisted nucleic acid amplification. This design can transduce the specific binding events between the aptamer and PTK7 protein into dramatically improved SERS signals. We have demonstrated ultrasensitive detection of PTK7 protein in the solution or on the target cell membrane directly. A mixture sample of 1000 cancer cells spiked into millions of blood cells can reliably be detected by the ACCESS assay without any requirement of enrichment. This work represents the first demonstration of detection of membrane protein biomarkers on living cells using enzyme assisted SERS technology with high performance. This new platform promises a useful and robust tool for important applications of in vitro diagnosis of the cancer cells and translational research of membrane protein biomarkers.[10,32−34]

EXPERIMENTAL SECTION

Chemicals. All chemicals in our experiments were of analytical grade and used without further purification. Aqueous solutions were prepared using deionized water (≥18 MΩ, Milli Q, Millipore). The SERS substrates were provided by Nanova Inc. (Columbia, MO, USA). Oligonucleotides were synthesized and HPLC purified by Sangon Biotech. The oligonucleotide sequences are listed in Table 1.

Electrophoresis Experiment. Agarose gel electrophoresis was performed by referring to the standard protocol in order to verify the Exo III assisted cleavage of the probe DNA. Agarose (2%, w/w) in the buffer of 1× TBE was used to test different DNA samples, including the probe DNA (P), the probe DNA and Exo III (P + Exo III), the bait DNA (T), the residual DNA (R), the probe and bait DNAs (P + T), and the mixture of the probe DNA, the bait DNA, and Exo III (P + T + Exo III), under the voltage of 110 V for 25 min.

Cell Culture and Treatment. CCRF CEM (human leukemia) and THP 1 (human acute monocytic leukemia) cells were cultured in RPMI 1640 cell medium, supplemented with 10% fetal bovine serum (FBS) and 1% penicillin/streptomycin at 37 °C and 5% CO_2 atmosphere. The cells were collected and centrifuged at 1000 rpm for 3 min in culture medium, washed twice with phosphate buffered saline (PBS) buffer, and then used for the subsequent tests of membrane protein detection. The cell density was determined by a hemacytometer.

Blood Sample Collection. Blood samples were collected from a healthy donor, according to the Guidelines for Safe Work Practices approved by the Committee on Ethics of Human Specimens and Animal Experiments at Soochow University. Tubes containing the anticoagulant (EDTA) were used for the blood samples. The blood cells, including both red and white blood cells, were obtained after removal of the upper plasma layer by centrifugation at 1500*g* for 15 min at room temperature. They were resuspended in RPMI 1640 medium (no FBS) for cell counting, followed by mixing with the spiked cancer cells.

Table 1. List of the Oligonucleotide Sequences in the Experiments

Oligonucleotides	Sequence (5' → 3')
Anglerfish aptamer (A)	ATCTAACTGCTGCGCCGCCGGGAAAATACTG
	TACGGTTAGATTTTTTTTTTTTTCAGCAGTTA
	GGAGAATTTAA
Probe DNA (P)	Cy5-AAAAGAGAATGGGTAGGGCGGGTTGGG
	CCCATTCTCCTAACTGCTG
Capture DNA (C)	CATTCTCTTTTTATTTATATT-SH
Bait DNA (T)	CAGCAGTTAGGAGAATTTAA
Residual DNA (R)	AAAAGAGAATGGGTAGGGCGGGTTGGGCCC

ACCESS Reactions. Sensitive detection of cell membrane protein biomarkers such as PTK7 was achieved by ACCESS reactions in several sequential steps. The anglerfish aptamer was denatured at 95 °C for 2 min, followed by an annealing process to room temperature. Then, the aptamer solution (100 nM) and cell suspension were mixed together and incubated at 4 °C for 1 h, so that the recognition between the aptamer and PTK7 protein on the target cell membrane would induce the conformational change of the aptamer. The cells were centrifuged (1000*g* for 5 min) and washed with PBS solution twice. Next, the probe DNA (1 μM) and Exo III (50 U) were added and incubated with the cells at 37 °C for 1 h. The newly exposed DNA segment in the anglerfish aptamer by the conformational change hybridized the probe DNA, which initiated its cleavage by Exo III enzyme and produced the residual DNA. The Exo III assisted DNA cleavage can be performed in a cycled manner for signal amplification. Afterwards, the mixture was heated up to 75 °C for 10 min in order to inactivate the enzyme. It was incubated with the Au NPs@Si substrate containing the capture DNA on the surface at 37 °C for 2 h, followed by the readout of SERS signals. Three identical ACCESS reactions were tested on separate Au NPs@Si substrates in parallel (n = 3).

Negative Controls in ACCESS Reactions. A series of control experiments were performed to verify ACCESS reactions for cell membrane protein PTK7 detection, including (I) only CCRF CEM cell (4×10^5); (II) aptamer solution (100 nM); (III) aptamer (100 nM) and probe DNA (1 μM); (IV) aptamer (100 nM), probe DNA (1 μM), and CCRF CEM cell (4×10^5); (V) aptamer (100 nM), probe DNA (1 μM), and Exo III (50 U) and ; (VI) the product solution of CCRF CEM cell (4×10^5), aptamer (100 nM), probe DNA (1 μM), and Exo III (50 U). The control samples were in parallel incubated with identical Au NPs@Si substrates containing the capture DNA at 37 °C for 2 h before the SERS measurements.

Limit of Detection. The target cell suspension solutions were prepared in gradient concentrations. They were incubated with the aptamer (100 nM) at 4 °C for 1 h. Then, the cells were incubated with the probe DNA (1 μM) and Exo III (50 U) at 37 °C for 1 h before SERS measurements. CCRF CEM cell numbers were in the range from 10^6 cells down to 10^3 cells in the final reactions (400 μL).

Assay Specificity. The specificity of the ACCESS assay was investigated in two ways. First, the purified PTK7 protein samples (0.1 pg mL^{-1}) and two negative control proteins including bovine serum albumin (BSA, 0.1 pg mL^{-1}) and human serum albumin (HSA,

0.1 pg mL^{-1}) were tested in parallel under identical condition. Second, SERS signals were compared between CCRF CEM cells and blood cells under identical condition. A series of cell samples were prepared by mixing 10^3 CCRF CEM cells and blood cell in a series ratio of 1:1, 1:10, 1:100, and 1:1000, and then tested by the same detection procedure.

Collection of Clinical Samples and Tests. Bone marrow biopsies from leukemia patients (n = 9) and healthy donors (n = 3) were collected and numbered, with individual informed consent forms in the Department of Hematology, the First Affiliated Hospital of Soochow University. The Ethics Committee of the First Affiliated Hospital of Soochow University approved the study as well as contents of the informed consent. After gradient centrifuge with lympholyte H cell separation media (Cedarlane Laboratories, Burlington, NC, USA), the nucleated cells were collected for subsequent tests. In flow cytometry experiments, the cells (2×10^5 cells/mL) were incubated with the Cy5 labeled sgc8 aptamer (1 μM) at 4 °C for 2 h. The cell samples were centrifuged (1000g for 3 min) and washed with PBS solution twice at room temperature. They were resuspended with PBS to perform flow cytometry analysis (Calibur, Becton Dickinson). Identical aliquots of the clinical samples were treated with the procedure as previously described for the ACCESS assays.

RESULTS AND DISCUSSION

Working Principle of the ACCESS Technology. The ACCESS technology is designed as a SERS based sensing platform for highly sensitive detection of a wide range of analytes including cell membrane surface protein biomarkers. It integrates the specific membrane protein triggered con formation change of the aptamer and the Exonuclease III assisted signal amplification in SERS technology (Scheme 1). PTK7 was chosen for our demonstration because it is an important protein biomarker, which has been reported to be aberrantly expressed in multiple cancers.[16,33] In this design, a DNA hairpin structure (Scheme 1a) is composed of a regular sgc8 aptamer strand (green)[28,35] for specific recognition of PTK7, a poly T DNA linker (blue), and a "bait" DNA segment (red, abbreviated as "T"). This hybrid DNA hairpin nanostructure can take the conformational change to recognize the target protein biomarker and behave itself in a way similar to an "anglerfish", thus being abbreviated as the "anglerfish aptamer" in the legend of Scheme 1. In the absence of PTK 7 protein, it keeps a stable stem loop structure (conformation A), with the "bait" DNA segment covered by the stem structure. When the anglerfish aptamer approaches the PTK7 protein on the cell membrane, the high binding affinity between the aptamer and PTK7 will induce a conformation change of the aptamer, leading to exposure of the "bait" DNA segment in the single stranded mode (conformation B) for subsequent amplification (Scheme 1b,c).

Scheme 1. Illustration of Aptamer Conformation Cooperated Enzyme Assisted SERS (ACCESS) Technology for the Detection of PTK7 Biomarker on the Surface of Live Cells; (a) Anglerfish Aptamer; (b) Recognition between the Aptamer and PTK7 Protein; (c) Zoomed in View of the Conformation Change due to the Recognition Event on the Cell Membrane; (d) Exo III Assisted Cleavage of the Probe DNA, While Recycling the "Bait" DNA Segment of the Anglerfish Aptamer; (e) SERS Detection of the Residual DNA after the Cleavage. Note: The "Bait" DNA (T, Shown in Red) Segment is Not Cleaved Away from the Anglerfish Aptamer by Exo III Enzyme. For the Purpose of Simplification, Only the Exposed T Segment, Instead of the Whole Aptamer, is Illustrated in the Step of Recycling with Exo III Cleavage Reaction (d)

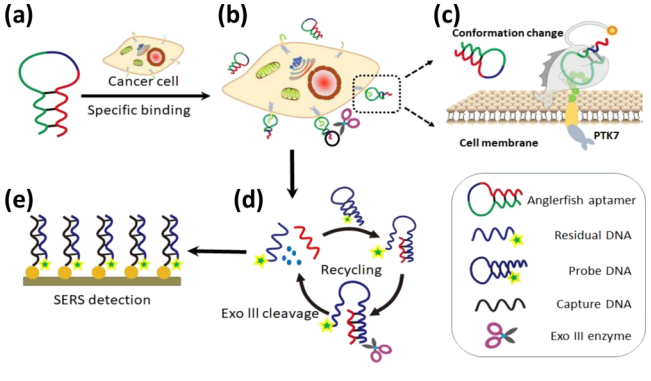

The probe DNA is designed as a stem loop oligonucleotide tagged with cyanine dye Cy5 at the 5′ end, containing the complementary sequence against the "bait" DNA segment of the anglerfish aptamer (Scheme 1d). It keeps a stem loop structure featuring a protrusion of the 3′ end when the "bait" DNA is in its covered conformation, thus free from digestion by the Exo III enzyme.[36,37] In contrast, the "bait" DNA in its exposed conformation can hybridize with probe DNA by opening its original stem loop structure and rebuilding the double strands with a blunt 3′ terminus. To draw an analogy, these interesting events technically build a scenario of the prey (the probe DNA) biting the hook (the "bait" DNA) set up by the anglerfish aptamer. Our ACCESS assay recruits the Exo III enzyme to cleave the probe DNA by starting with the blunt 3′ terminus. The cleavage is performed continuously to remove mononucleotides in a stepwise manner until the generation of a single stranded residual DNA out of the probe. In the meantime, the "bait" DNA is released intact in its exposed conformation, being available to initiate another cycle of probe DNA cleavage, which allows the anglerfish aptamer to catch a new prey. Consequently, a single copy of the exposed "bait" DNA segment in the anglerfish aptamer can take part in many cycles of the cleavage reaction with the assistance of Exo III, generating multiple copies of the residual DNA (Scheme 1d). This amplification process intensively promotes the SERS signals when the Cy5 tagged residual DNAs hybridize the capture DNAs on the Au NPs@Si substrate (Scheme 1e). The strategy of ACCESS highlights an integration of two important characteristics: (1) aptamer conformation cooperated change for exposure of the "bait" DNA; (2) Exo III assisted cleavage of the probe DNA for SERS signal amplification by multiple cycled hybridization and release of the "bait" DNA.

Consequently, it brings the advantages such as high sensitivity, selective detection of the target biomarker, and signal on readout. The ACCESS technology is flexible to be adapted for the detection of many other protein biomarkers due to the introduction of the independent "bait" DNA segment fused with an interchangeable aptamer sequence on demand. It allows for the detection of the target protein biomarkers on the surface of live cells, without the requirement of cell lysis. The benefits include minimizing the undesired mixture derived from the cell membrane and cell plasma, or from the contaminated cell lysates of nontargeted cells, thus reducing the interference of background noise. It is also beneficial to the biomedical applications, which request recovery of the live cells for further investigation on cell proliferation, migration, or drug screening.

The sequence optimization of DNA oligos in the ACCESS technology was performed by a theoretical analysis for their minimum free energy (MFE) secondary structures (Figure 1) and hybridization efficiencies in silica (Figures S1 and S2) using the online software suite, NUPACK.[38]

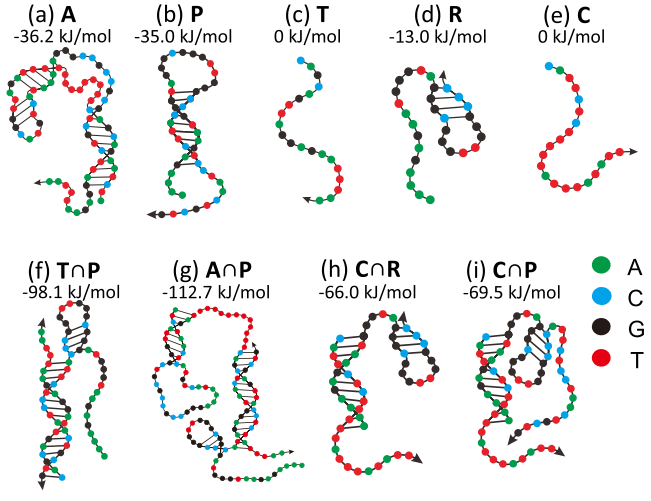

Figure 1. MFE structures of different oligos (a–e, oligo A, P, T, R, and C) and oligo hybridization with annotation of free energy calculated by NUPACK (f–i, T∩P, A∩P, C∩R, C∩P). Abbreviations: Anglerfish aptamer (A); the probe DNA (P); the bait DNA (T); the residual DNA (R); the capture DNA (C). ∩ symbols hybridization of the oligos.

Preparation and Characterization of the Substrates for SERS. As shown in Figure 2a,b, gold nanoparticles (Au NPs, 60 nm on the average) were densely coated on the surface of silicon wafers, exhibiting a wafer scaled uniform distribution. Single stranded capture DNAs were immobilized on the substrate surface via the Au–S bonds. The dramatic change in the contact angle measurements before (θ = 82°) and after (θ = 25°) incubation (Figure S3) was attributed to the hydrophilic phosphate groups of the DNA strand, indicating successful immobilization of the capture DNA on the substrate surface.

The Au NPs@Si substrate produced much stronger SERS signals than the control of using pure silicon wafer (Figure 2e), using a standard dye (R6G). The enhanced factor (EF) value[39] of Au NPs@Si substrate was calculated to be 1.95×10^6. We investigated the reproducibility of the Au NPs@Si substrates by recording both the spot to spot and the chip to chip variations. As shown in Figure 2f, the SERS spectra from 50 randomly selected spots on a single substrate exhibited quite uniform profiles, featuring a small relative standard deviation (RSD) value of 12% (calculated using the peak intensities at 1364 cm^{-1} of R6G). We validated that the SERS signals were highly reproducible by measuring the chip to chip variations of four separate substrates (RSD 9–14% Figure S4).

Validation of Exo III Enzymatic Cleavage and ACCESS Assay. The reaction of Exo III enzymatic cleavage of the probe DNA was verified using the standard agarose gel electrophoresis. As shown in Figure S5, there was no change for the probe DNA (P) with or without incubation of the Exo III enzyme (column 1 and 2), indicating that the stem loop secondary structure of the probe DNA was relatively stable and resistant to enzyme digestion before its conformational change. The gel electrophoresis experiment included two oligonucleotides with the sequences of the bait DNA segment (T in column 3) and the residual DNA segment (R in column 4) as the references. After P hybridized with T, the band of the product (T∩P, column 5) moved toward the higher number of base pairs as expected in comparison with the previous band (P in column 1). However, incubation of T∩P with the Exo III enzyme generated a band back to the lower number of base pairs, identical to the residue DNA (column 4). The results suggested that the characteristic Exo III enzymatic cleavage of P was successfully triggered by the hybridization with T (T∩P) to form a blunt 3′ end according to our design.

The feasibility of the ACCESS assay was further validated using a series of control samples for the SERS measurements. As shown in Figure 3a, there was a distinct difference of the SERS signal intensity between the positive experiments and negative controls. The characteristic SERS signals of Cy5 were produced on the Au NPs@Si substrate in the positive sample (Figure 3a, curve VI, containing the aptamer/probe/CCRF CEM cell and Exo III). In contrast, only background noise was observed in the negative control groups, including the CCRF CEM cell suspension (curve I), the aptamer (curve II), the aptamer/probe DNAs (curve III), the aptamer/probe/CCRF CEM cell without Exo III enzyme (IV), and the aptamer/probe plus Exo III enzyme (V). The background noise level in the control V was slightly elevated compared to the other control groups (I–IV), which might be caused by a minor side reaction related to the aptamer and the probe DNA. Quantitative analysis of the SERS spectra at the 1366 cm^{-1} peak (Figure 3b) suggested that the signal intensity of the positive sample (VI) was 4–5 folds higher than in the control (V), or nearly 15 folds higher than the other controls (I–VI). The assay reproducibility was evaluated by profiling the SERS spectra of Cy5 from 50 random spots on the substrate in the positive experiment (VI). As shown in Figure 3c, the SERS spectra were overall quite uniform. The detailed signal intensities at the characteristic peak of 1366 cm^{-1} from the spot panel are presented in Figure 3d. They confirmed the high reproducibility of the ACCESS assay with a relatively low signal variation (RSD value of 12.1%).

Ultrasensitive Detection of PTK7 on the Surface of Living Cells. We optimized the ACCESS assay by titrating the important parameters in the enzyme assisted amplification. The optimal conditions were determined to include the final concentration of the probe DNA (1 μM), the concentration of Exo III enzyme (50 units per assay), and the reaction time (60 min) (Figure S6). The sensitivity of the ACCESS assay was investigated by testing different concentrations of the target CCRF CEM cells ranging from 10^6 to 10^3 cells per assay. As shown in Figure 4a, a series of SERS spectra were collected, exhibiting a trend of the signal intensity dependent on the target cell number. Quantitative analysis suggested that the intensities of the characteristic SERS peak of Cy5 at 1366 cm^{-1} was reduced from 6×10^3 to 2.6×10^3, along with the cell dilution from 10^6 to 10^3 cells per assay (Figure 4b). A good linearity (correlation coefficient, R^2 = 0.983) covered 3 orders of magnitude of the cell concentration range (Figure S7). The LOD of the ACCESS assay was determined to be as low as dozens of the CCRF CEM cells by extrapolating the line of cell titration experiments to the standard requirement of signal to noise ratio (S/N = 3) in Figure S7.

We attempted to compare the performance of our ACCESS assay with a commercial ELISA kit for the detection of PTK7 proteins on the cell surface. ELISA is traditionally an important

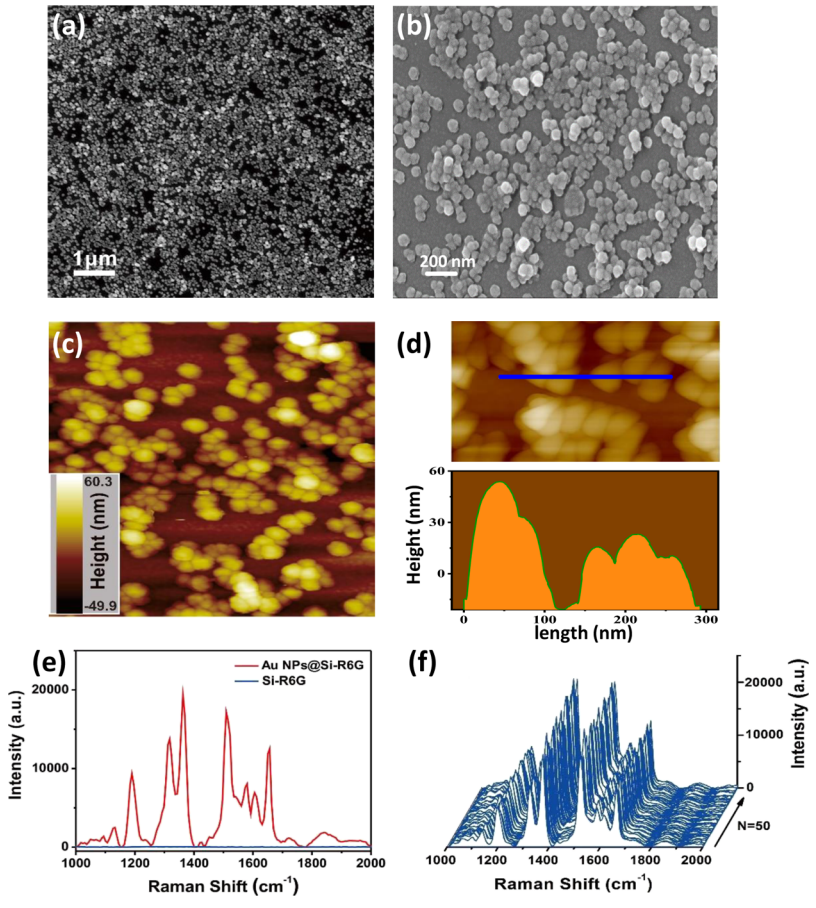

Figure 2. The characterization of the Au NPs@Si substrate for the ACCESS assay. (a,b) Scanning electron microscopy images in different magnifications. Scale bar as specified. (c,d) Atomic force microscopy images in different magnifications, including the profile of the Au nanostructures along the blue line on the substrate surface. Scale bar as measured. (e) SERS spectra of the standard dye molecules (R6G) on the Au NPs@Si substrate (red, 1 μM) or the silicon wafer (blue, 10 mM). (f) SERS spectra of R6G collected from 50 random spots on a single Au NPs@Si substrate, demonstrating reproducible spot to spot performance.

immunoassay to detect various disease protein biomarkers and pathogens with the LOD down to subnano gram per mL.[20] The detection range of the commercial ELISA kit for PTK7 was determined by the experiments according to the manufacturer's protocol, exhibiting a good linearity (R^2 = 0.995) between the absorbance change and PTK7 concen trations from 12.5 to 200 pg mL^{-1} (Figure S8a). The expression level of PTK7 proteins on the cell surface was calibrated by titrating the concentrations of CCRF CEM cells (Figure S8b). The LOD of the ELISA kit for living cells was determined to be 10^7 cell mL^{-1}. Below this cell concentration, the absorbance change by the ELISA kit was indistinguishable from the background noise of the blank control. Although the ELISA kit recruited the well established HRP enzyme technology for signal amplification, the LOD for the living cell samples by ELISA was still nearly 5 orders of magnitude inferior to that by the ACCESS assay. The comparison highlighted the capacity of the ACCESS assay in ultrasensitive detection of protein biomarkers due to synergistic integration of Exo III assisted amplification and SERS technology.

Besides CCRF CEM, another cell line (THP 1), human monocytes derived from a patient with acute monocytic leukemia, was included in our tests of ACCESS for comparison. We built a protocol to acquire the fluorescent images of these two cell lines after they were incubated with the Cy5 labeled sgc8 aptamer. As shown in Figure S9a, CCRF CEM and THP 1 were presented with good cell morphology. Both of them were successfully stained, exhibiting fluorescence in the channel of Cy5 on the cell surface. It suggested an elevated expression of PTK7 biomarkers in both of these two cell lines. Semiquantitative analysis of the fluorescent images indicated that the expression level of PTK7 on CCRF CEM cells might be higher than that on THP 1 cells (Figure S9b). The difference in PTK7 expression between these cell models was also observed in the results of the ACCESS assays (Figure S10a,b), demonstrating a potential application to discriminate leukemia cells in different forms or progression by this approach.

Specificity Evaluation of the ACCESS Assay. The specificity of the ACCESS assay was investigated by testing PTK7 protein against controls such as BSA and HSA. As shown in Figure 5a, there were intensive SERS signals of Cy5 characteristic peaks produced by the ACCESS assay for the target analyte of PTK7 protein, whereas no detectable SERS signals for the negative controls of BSA or HSA. The results demonstrated a high specificity of the ACCESS assay in the identification of PTK7 against other potential contaminants, thanks to the integration of the selective aptamer and a careful design of the oligo sequences. In addition, the ACCESS assay was applied to test different types of cell samples such as CCRF CEM cells and human blood cells (including both the red blood cells and white blood cells) in a series of dilutions

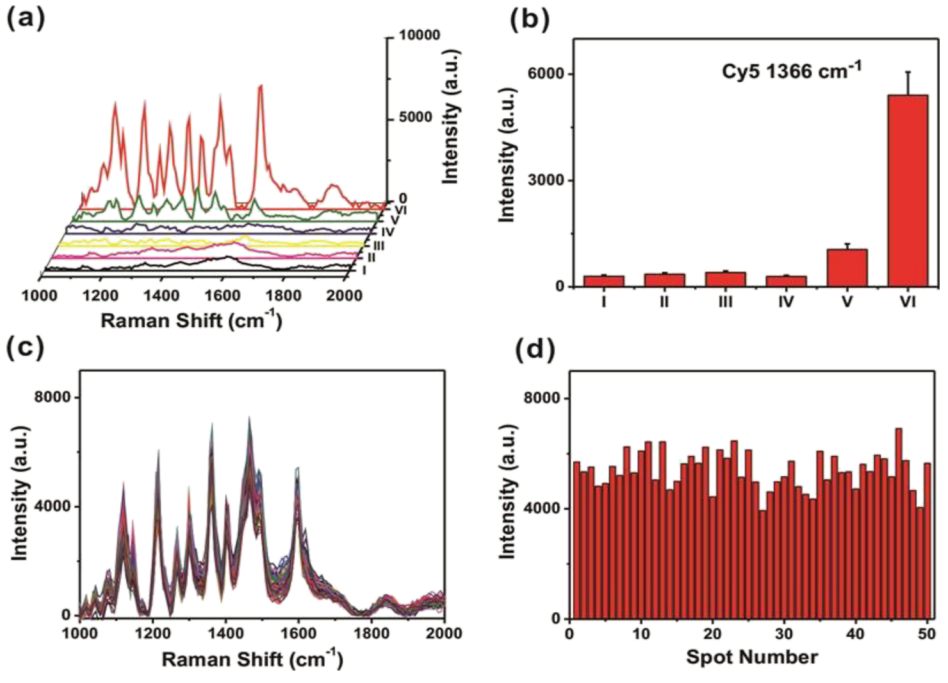

Figure 3. Validation of the ACCESS assay by SERS measurements. (a) SERS spectra of a series of control samples on the Au NPs@Si substrates immobilized with the capture DNA. (b) Intensity quantification of the SERS signals at 1366 cm^{-1} peak. Sample I: CCRF CEM cell. II: aptamer. III: aptamer and probe DNA. IV: aptamer, probe DNA, and CCRF CEM cell. V: aptamer, probe DNA, and Exo III. VI: aptamer, probe DNA, Exo III, and CCRF CEM cell. Error bars: standard deviation from three independent assays (n = 3). (c) SERS spectra of testing CCRF CEM cell collected from 50 random spots on the Au NPs@Si substrate in a single assay. Cell number: 4×10^5 per assay. (d) SERS intensity profile at 1366 cm^{-1} peak from the 50 random spots, corresponding to the data in (c).

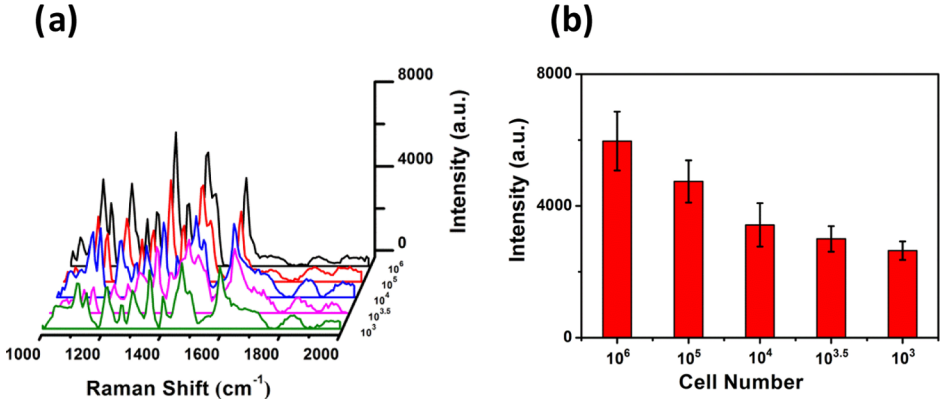

Figure 4. Sensitive detection of PTK7 on the surface of live CCRF CEM cells by ACCESS assays. (a) SERS spectra of titrating the target cell number from 10^6 to 10^3 cells per assay. (b) Intensity quantification of the SERS signals at 1366 cm^{-1} peak in the titration experiments. Error bar: standard deviation (n = 3).

(Figure 5b). The SERS signal intensities on the CCRF CEM cells were dependent on cell concentrations, which were significantly higher than the blood cells in all of the concentration gradient. Importantly, the concentration changes of the blood cells did not influence the background noise level, suggesting that the ACCESS assay was free from the interference by the nontarget cell concentrations. Therefore, a potential application of the ACCESS assay includes the detection of circulating tumor cells (CTCs). As a special group of rare cells shedding from primary tumors and freely circulating in the blood, CTCs retain the ability to initiate metastasis and form secondary tumors in distant organs.[40−42] Therefore, CTCs have been proposed as the critical biomarkers from liquid biopsies to monitor metastatic relapse and therapeutic management.[43,44] Detection of CTCs is challenging not only because of the extremely low abundance of CTCs (<10^2 cell mL^{-1}), but also the complicated noise interference from various types of the blood cells in the clinical samples.[45−49] We attempted to examine the samples in a series of premixing ratios (1:1, 1:10, 1:100, and 1:1000) between the CCRF CEM cells and the blood cells, in order to further evaluate the specificity of the ACCESS assay. As shown in Figure 5c,d, the increase of the nontarget blood cells in the spiked samples did not compromise the SERS signals produced by the CCRF CEM cells, suggesting a great selectivity of the ACCESS assay in the detection of the membrane protein biomarkers on live cells.

ACCESS Assays on the Clinical Samples. A pilot study was performed to evaluate the utility of the ACCESS assay for potentially clinical practice. Bone marrow biopsies were

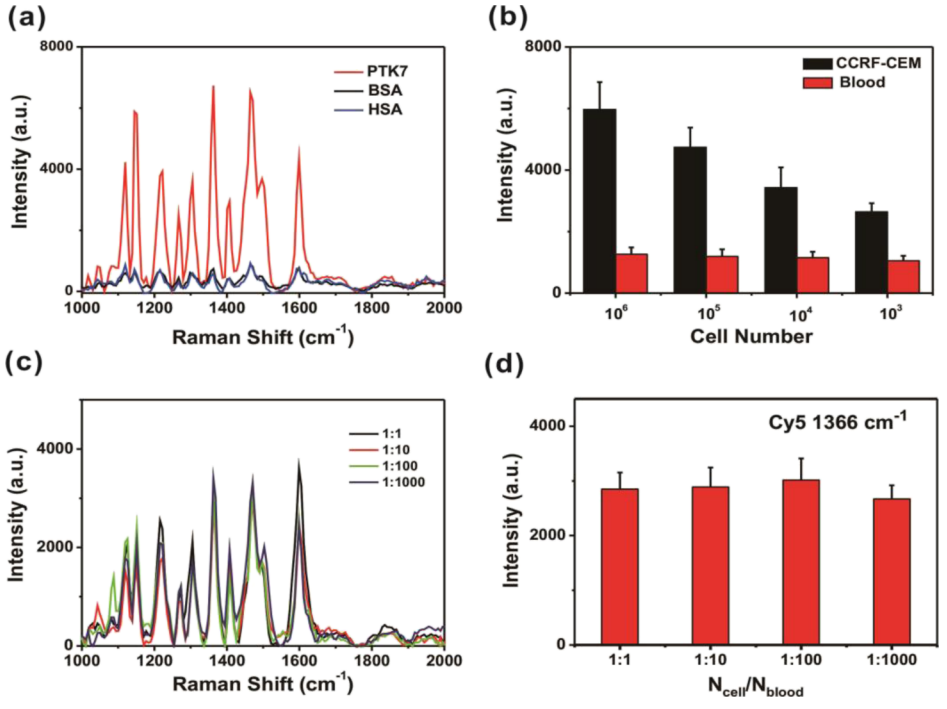

Figure 5. Specificity evaluation of ACCESS assays for the detection of PTK7. (a) SERS spectra of different protein samples on the substrates, including PTK7 and the negative controls of BSA and HAS, protein concentration: 0.1 mg mL^{-1}. (b) Intensity quantification of the SERS signals at 1366 cm^{-1} peak in testing the cell samples (CCRF CEM cells and human blood cells separately) with different cell number per assay as specified. Error bar: standard deviation (n = 3). (c) SERS spectra of testing the mixtures of CCRF CEM cells and human blood cells in a series of dilution ratios. (d) Intensity quantification of the SERS signals at 1366 cm^{-1} peak in testing the mixed cell samples, corresponding to the data in (c). Error bar: standard deviation (n = 3).

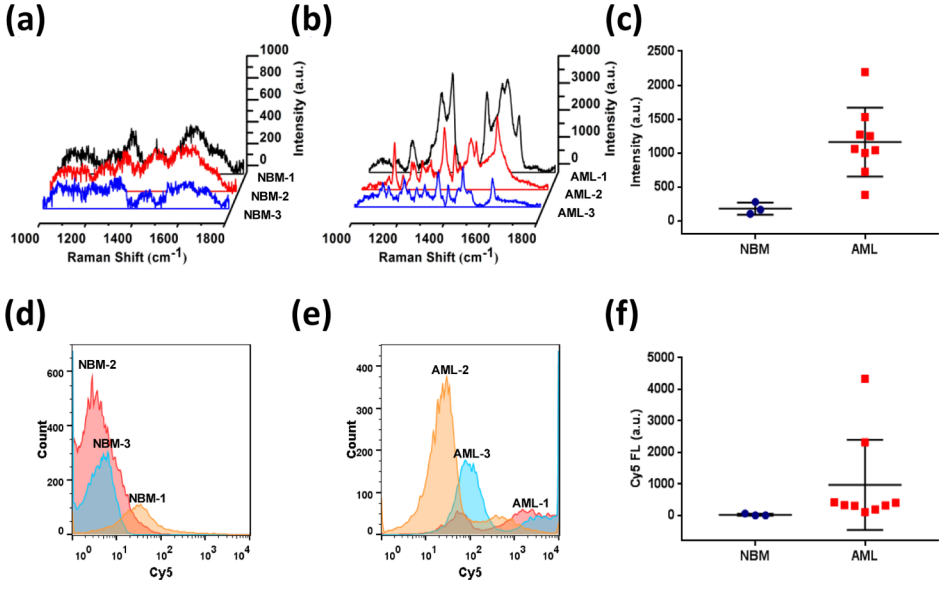

Figure 6. The tests on the clinical samples (bone marrow biopsies) by ACCESS and flow cytometry. (a,b) SERS spectra of the samples by ACCESS, including three healthy donors (NBM1−3) and three patients (AML1−3). (c) Comparison of the healthy donor group (n = 3) and AML patient group (n = 9) by ACCESS. (d,e) Event counting of the samples by flow cytometry, including three healthy donors (NBM1−3) and three patients (AML1−3). (f) Comparison of the healthy donor group (n = 3) and AML patient group (n = 9) by the flow cytometry. The samples in the tests of flow cytometry were incubated with the Cy5 labeled sgc8 aptamer (1 μM) at 4 °C for 2 h.

collected from nine patients who had been diagnosed with AML, as well as from three healthy donors. These clinical samples were tested with the ACCESS assay (Figure 6a−c). As the negative controls, there were no identifiable SERS peaks in the spectra tested using any samples from the three healthy donors (Figure 6a). In contrast, all of the tests using the individual samples from the nine AML patients produced positive SERS signals by the ACCESS method. Among them, the spectra of three representative AML patient cases are displayed in Figure 6b. We performed quantitative analysis of the characteristic SERS peak intensities of Cy5 at 1366 cm^{-1} for all samples, which suggested a 5 fold or 6 fold difference in

the mean values between the AML patient group and healthy donor group (Figure 6c). Based on the data by the ACCESS assays, the difference between the individual cases was relatively small in the healthy donor group. It became much wider in the AML patient groups probably because of different extents of disease progression (Figure 6c).

Flow cytometry experiments were in parallel performed on identical aliquots of the clinical samples after an incubation step for the cells to be recognized by the Cy5 labeled sgc8 aptamer. As shown in Figure 6d,e, the cellular profiles were distinctly different between the bone marrow samples from the healthy donors and AML patients. The cell fluorescent intensities by Cy5 labeling from the healthy donors were in the range of zero to dozens of arbitrary units, much lower than those from AML patients. Quantitative data analysis of the flow cytometry experiments verified the difference in Cy5 fluorescence between these two groups (Figure 6f). Detailed comparison between the ACCESS and flow cytometry data suggested an excellent correlation between individual samples case by case, supporting reliable performance by the ACCESS assay (Table S1).

The ACCESS technology may find important applications such as minimal residue disease (MRD) diagnosis.[50] In the previous clinical studies of childhood or adult ALL, the role of MRD monitoring has been highlighted as the strongest prognostic factor for stratification of risk group assignment and treatment choices.[50,51] The development of MRD techniques must be sensitive, broadly applicable, accurate, reliable, fast, and affordable in order to meet the requirements of clinical utilization.[50] There is still a gap between ACCESS sensitivity with the current setting up ($\leq 10^{-3}$) and MRD diagnostics requirement ($\leq 10^{-4}$). It can be fulfilled by improvement of the EF value of the SERS substrates (currently 1.95×10^{6}) by several orders of magnitude (EF up to 1×10^{13}) with new nanofabrication techniques.[52] Our experiments suggest an accurate and reliable performance of the ACCESS assay, by testing different types of samples such as cell lines, spiked blood samples, and bone marrow biopsies. The crucial steps of the ACCESS assay takes a few hours in total, including Exo III amplification and DNA hybridization, which is comparable to the standard MRD diagnostic techniques.[50] Further development of ACCESS with improvements in SERS substrate choices and larger scale of clinical tests will help translating this new technique onto MRD diagnostic applications.

CONCLUSIONS

In summary, we have developed a new biosensor for membrane protein (PTK7) on live cells using aptamer conformation cooperated enzyme assisted SERS (ACCESS) technology. This strategy of integrating SERS, aptamer, and highly efficient amplification by the Exo III enzyme enables more sensitive detection of the target tumor cells (CCRF CEM) than the commercial ELISA method by several orders of magnitude. The ACCESS assay exhibits an excellent specificity in differentiating between the target cells (CCRF CEM) and normal blood cells. Our approach features a signal on detection mechanism and no requirement for cell lysis or sample prepurification steps, thus offering a flexible platform to detect membrane protein biomarkers on live cells for medical research and early clinical diagnostics.

ASSOCIATED CONTENT

Supporting Information

The Supporting Information is available free of charge on the ACS Publications website at DOI: 10.1021/acssensors.9b00604.

Supplementary details for the experimental section, theoretical calculations of the energy changes for the competitive hybridizations between DNA oligos, contact angle measurements, SERS spectra for chip to chip reproducibility, agarose gel electrophoresis, optimization for the ACCESS assay, linear fitting of the titration curves, detection using a commercial ELISA kit as the control, confocal laser scanning microscopic images and ACCESS data for different cell lines, and table of the tests on the clinical samples (PDF)

AUTHOR INFORMATION

Corresponding Author

*E mail: jliu@suda.edu.cn. iMINTS Lab: http://web.suda.edu.cn/jliu/.

ORCID

Michael Hirtz: 0000 0002 2647 5317

Jian Liu: 0000 0002 0095 8978

Author Contributions

Y.L., Q.F., and X.M. contributed equally to this manuscript. J.L. and Y.L. conceived and designed the experiments. Y.L., Q.F., and X.M. participated in DNA probe designs/optimization and SERS measurements. X.Z. and Y.Z. provided help in collecting the clinical samples and analyzing the flow cytometry data. J.Y., Y.Z., and R.W. provided help in confocal fluorescent imaging and gel electrophoresis. J.L., Y.L., and M.H. wrote the manuscript. B.N. participated in discussions of writing.

Notes

The authors declare no competing financial interest.

ACKNOWLEDGMENTS

This work was supported by the National Key Research and Development Program of China (2017YFE0131700) and by the National Natural Science Foundation of China (21575095, 21874096); a project supported by Collaborative Innovation Center of Suzhou Nano Science and Technology, the 111 Project, and the Priority Academic Program Development (PAPD) of Jiangsu Higher Education Institutions.

REFERENCES

(1) Schirmer, E. C.; Florens, L.; Guan, T. L.; Yates, J. R.; Gerace, L. Nuclear membrane proteins with potential disease links found by subtractive proteomics. *Science* **2003**, *301*, 1380−1382.

(2) Gusterson, B. A.; Warburton, M. J.; Mitchell, D.; Ellison, M.; Neville, A. M.; Rudland, P. S. Distribution Of Myoepithelial Cells And Basement Membrane Proteins In the Normal Breast And In Benign And Malignant Breast Diseases. *Cancer Res.* **1982**, *42*, 4763−4770.

(3) Sanders, C. R.; Myers, J. K. Disease related misassembly of membrane proteins. *Annu. Rev. Biophys. Biomol. Struct.* **2004**, *33*, 25−51.

(4) Hartzell, H. C.; Qu, Z.; Yu, K.; Xiao, Q.; Chien, L. T. Molecular physiology of bestrophins: Multifunctional membrane proteins linked to best disease and other retinopathies. *Physiol. Rev.* **2008**, *88*, 639−672.

(5) Fry, M. Y.; Clemons, W. M. Complexity in targeting membrane proteins. *Science* **2018**, *359*, 390−391.

(6) Gärtner, S.; Gunesch, A.; Knyazeva, T.; Wolf, P.; Högel, B.; Eiermann, W.; Ullrich, A.; Knyazev, P.; Ataseven, B. PTK 7 Is a Transforming Gene and Prognostic Marker for Breast Cancer and Nodal Metastasis Involvement. *PLoS One* **2014**, *9*, No. e84472.
(7) Mossie, K.; Jallal, B.; Alves, F.; Sures, I.; Plowman, G. D.; Ullrich, A. Colon Carcinoma Kinase 4 Defines a New Subclass Of the Receptor Tyrosine Kinase Family. *Oncogene* **1995**, *11*, 2179−2184.
(8) Park, S. K.; Lee, H. S.; Lee, S. T. Characterization of the human full length PTK7 cDNA encoding a receptor protein tyrosine kinase like molecule closely related to chick KLG. *J. Biochem.* **1996**, *119*, 235−239.
(9) Berger, H.; Wodarz, A.; Borchers, A. PTK7 Faces the Wnt in Development and Disease. *Front. Cell Dev. Biol.* **2017**, *5*, 31.
(10) Katoh, M. Antibody drug conjugate targeting protein tyrosine kinase 7, a receptor tyrosine kinase like molecule involved in WNT and vascular endothelial growth factor signaling: effects on cancer stem cells, tumor microenvironment and whole body homeostasis. *Ann. Transl. Med.* **2017**, *5*, 462.
(11) Lander, R.; Petersen, C. P. Wnt, Ptk7, and FGFRL expression gradients control trunk positional identity in planarian regeneration. *eLife* **2016**, *5*, No. e12850.
(12) Haines, C. J.; Giffon, T. D.; Lu, L. S.; Lu, X.; Tessier Lavigne, M.; Ross, D. T.; Lewis, D. B. Human CD4(+) T cell recent thymic emigrants are identified by protein tyrosine kinase 7 and have reduced immune function. *J. Exp. Med.* **2009**, *206*, 275−285.
(13) Liu, Y.; Chen, J.; Sethi, A.; Li, Q. K.; Chen, L.; Collins, B.; Gillet, L. C. J.; Wollscheid, B.; Zhang, H.; Aebersold, R. Glycoproteomic Analysis of Prostate Cancer Tissues by SWATH Mass Spectrometry Discovers N acylethanolamine Acid Amidase and Protein Tyrosine Kinase 7 as Signatures for Tumor Aggressiveness. *Mol. Cell. Proteomics* **2014**, *13*, 1753−1768.
(14) Linger, R. M.; Keating, A. K.; Earp, H. S.; Graham, D. K. Taking aim at Mer and Axl receptor tyrosine kinases as novel therapeutic targets in solid tumors. *Expert Opin. Ther. Targets* **2010**, *14*, 1073−1090.
(15) Shin, W. S.; Kwon, J.; Lee, H. W.; Kang, M. C.; Na, H. W.; Lee, S. T.; Park, J. H. Oncogenic role of protein tyrosine kinase 7 in esophageal squamous cell carcinoma. *Cancer Sci.* **2013**, *104*, 1120−1126.
(16) Jiang, G.; Zhang, M.; Yue, B.; Yang, M.; Carter, C.; Al Quran, S. Z.; Li, B.; Li, Y. PTK7: A new biomarker for immunophenotypic characterization of maturing T cells and T cell acute lymphoblastic leukemia. *Leuk. Res.* **2012**, *36*, 1347−1353.
(17) Meng, L.; Sefah, K.; O'Donoghue, M. B.; Zhu, G.; Shangguan, D.; Noorali, A.; Chen, Y.; Zhou, L.; Tan, W. Silencing of PTK7 in Colon Cancer Cells: Caspase 10 Dependent Apoptosis via Mitochon drial Pathway. *PLoS One* **2010**, *5*, No. e14018.
(18) Jacobson, O.; Weiss, I. D.; Wang, L.; Wang, Z.; Yang, X.; Dewhurst, A.; Ma, Y.; Zhu, G.; Niu, G.; Kiesewetter, D. O.; Vasdev, N.; Liang, S. H.; Chen, X. 18F Labeled Single Stranded DNA Aptamer for PET Imaging of Protein Tyrosine Kinase 7 Expression. *J. Nucl. Med.* **2015**, *56*, 1780−1785.
(19) Lázaro, I.; Gonzalez, M.; Roy, G.; Villar, L. M.; Gonzalez Porqué, P. Description Of an Enzyme Linked Immunosorbent Assay for the Detection Of Protein Tyrosine Kinase. *Anal. Biochem.* **1991**, *192*, 257−261.
(20) Lin, Y.; Zhang, L. H.; Wang, X. H.; Xing, X. F.; Cheng, X. J.; Dong, B.; Hu, Y.; Du, H.; Li, Y. A.; Zhu, Y. B.; Ding, N.; Du, Y. X.; Li, J. Y.; Ji, J. F. PTK7 as a novel marker for favorable gastric cancer patient survival. *J. Surg. Oncol.* **2012**, *106*, 880−886.
(21) Yin, Y.; Mitson Salazar, A.; Prussin, C. Detection of Intracellular Cytokines by Flow Cytometry. *Curr. Protoc. Immunol.* **2015**, *110*, 6.24.1−18.
(22) Cordes, R. J.; Ryan, M. E. Pitfalls in HIV testing. *Postgrad. Med.* **1995**, *98*, 177−189.
(23) Dekker, E. L.; Porta, C.; Van Regenmortel, M. H. V. Limitations Of Different Elisa Procedures for Localizing Epitopes In Viral Coat Protein Subunits. *Arch. Virol.* **1989**, *105*, 269−286.
(24) Hermann, T.; Patel, D. J. Adaptive Recognition by Nucleic Acid Aptamers. *Science* **2000**, *287*, 820−825.
(25) Li, F.; Zhang, H.; Wang, Z.; Newbigging, A. M.; Reid, M. S.; Li, X. F.; Le, X. C. Aptamers Facilitating Amplified Detection of Biomolecules. *Anal. Chem.* **2015**, *87*, 274−292.
(26) Ma, H.; Liu, J.; Ali, M. M.; Mahmood, M. A. I.; Labanieh, L.; Lu, M.; Iqbal, S. M.; Zhang, Q.; Zhao, W.; Wan, Y. Nucleic acid aptamers in cancer research, diagnosis and therapy. *Chem. Soc. Rev.* **2015**, *44*, 1240−1256.
(27) Feagin, T. A.; Maganzini, N.; Soh, H. T. Strategies for Creating Structure Switching Aptamers. *ACS Sens.* **2018**, *3*, 1611−1615.
(28) Shangguan, D.; Cao, Z.; Meng, L.; Mallikaratchy, P.; Sefah, K.; Wang, H.; Li, Y.; Tan, W. Cell specific aptamer probes for membrane protein elucidation in cancer cells. *J. Proteome Res.* **2008**, *7*, 2133−2139.
(29) Lin, S.; Gao, W.; Tian, Z.; Yang, C.; Lu, L.; Mergny, J. L.; Leung, C. H.; Ma, D. L. Luminescence switch on detection of protein tyrosine kinase 7 using a G quadruplex selective probe. *Chem. Sci.* **2015**, *6*, 4284−4290.
(30) Zhou, N.; Su, F.; Guo, C.; He, L.; Jia, Z.; Wang, M.; Jia, Q.; Zhang, Z.; Lu, S. Two dimensional oriented growth of Zn MOF on Zr MOF architecture: A highly sensitive and selective platform for detecting cancer markers. *Biosens. Bioelectron.* **2019**, *123*, 51−58.
(31) Li, Y.; Zhao, Q.; Wang, Y.; Man, T.; Zhou, L.; Fang, X.; Pei, H.; Chi, L.; Liu, J. Ultrasensitive Signal On Detection of Nucleic Acids with Surface Enhanced Raman Scattering and Exonuclease III Assisted Probe Amplification. *Anal. Chem.* **2016**, *88*, 11684−11690.
(32) Prebet, T.; Lhoumeau, A. C.; Arnoulet, C.; Aulas, A.; Marchetto, S.; Audebert, S.; Puppo, F.; Chabannon, C.; Sainty, D.; Santoni, M. J.; Sebbagh, M.; Summerour, V.; Huon, Y.; Shin, W. S.; Lee, S. T.; Esterni, B.; Vey, N.; Borg, J. P. The cell polarity PTK7 receptor acts as a modulator of the chemotherapeutic response in acute myeloid leukemia and impairs clinical outcome. *Blood* **2010**, *116*, 2315−2323.
(33) Tian, X.; Yan, L.; Zhang, D.; Guan, X.; Dong, B.; Zhao, M.; Hao, C. PTK7 overexpression in colorectal tumors: Clinicopatho logical correlation and prognosis relevance. *Oncol. Rep.* **2016**, *36*, 1829−1836.
(34) Kelley, S. O. Advancing Ultrasensitive Molecular and Cellular Analysis Methods to Speed and Simplify the Diagnosis of Disease. *Acc. Chem. Res.* **2017**, *50*, 503−507.
(35) Shangguan, D.; Tang, Z.; Mallikaratchy, P.; Xiao, Z.; Tan, W. Optimization and modifications of aptamers selected from live cancer cell lines. *ChemBioChem* **2007**, *8*, 603−606.
(36) Henikoff, S. Unidirectional Digestion with Exonuclease III In DNA Sequence Analysis. *Methods Enzymol.* **1987**, *155*, 156−165.
(37) Mol, C. D.; Kuo, C. F.; Thayer, M. M.; Cunningham, R. P.; Tainer, J. A. Structure And Function Of the Multifunctional DNA Repair Enzyme Exonuclease III. *Nature* **1995**, *374*, 381−386.
(38) Zadeh, J. N.; Steenberg, C. D.; Bois, J. S.; Wolfe, B. R.; Pierce, M. B.; Khan, A. R.; Dirks, R. M.; Pierce, N. A. NUPACK: Analysis and Design of Nucleic Acid Systems. *J. Comput. Chem.* **2011**, *32*, 170−173.
(39) Durucan, O.; Rindzevicius, T.; Schmidt, M. S.; Matteucci, M.; Boisen, A. Nanopillar Filters for Surface Enhanced Raman Spectros copy. *ACS Sens.* **2017**, *2*, 1400−1404.
(40) Yu, M.; Stott, S.; Toner, M.; Maheswaran, S.; Haber, D. A. Circulating tumor cells: approaches to isolation and characterization. *J. Cell Biol.* **2011**, *192*, 373−382.
(41) Alix Panabieres, C.; Pantel, K. Circulating Tumor Cells: Liquid Biopsy of Cancer. *Clin. Chem.* **2013**, *59*, 110−118.
(42) Cristofanilli, M.; Budd, G. T.; Ellis, M. J.; Stopeck, A.; Matera, J.; Miller, M. C.; Reuben, J. M.; Doyle, G. V.; Allard, W. J.; Terstappen, L. W. M. M.; Hayes, D. F. Circulating tumor cells, disease progression, and survival in metastatic breast cancer. *N. Engl. J. Med.* **2004**, *351*, 781−791.
(43) Shen, Z.; Wu, A.; Chen, X. Current detection technologies for circulating tumor cells. *Chem. Soc. Rev.* **2017**, *46*, 2038−2056.

(44) Nagrath, S.; Sequist, L. V.; Maheswaran, S.; Bell, D. W.; Irimia, D.; Ulkus, L.; Smith, M. R.; Kwak, E. L.; Digumarthy, S.; Muzikansky, A.; Ryan, P.; Balis, U. J.; Tompkins, R. G.; Haber, D. A.; Toner, M. Isolation of rare circulating tumour cells in cancer patients by microchip technology. *Nature* **2007**, *450*, 1235−1239.
(45) Pantel, K.; Speicher, M. R. The biology of circulating tumor cells. *Oncogene* **2016**, *35*, 1216−1224.
(46) Karabacak, N. M.; Spuhler, P. S.; Fachin, F.; Lim, E. J.; Pai, V.; Ozkumur, E.; Martel, J. M.; Kojic, N.; Smith, K.; Chen, P. i.; Yang, J.; Hwang, H.; Morgan, B.; Trautwein, J.; Barber, T. A.; Stott, S. L.; Maheswaran, S.; Kapur, R.; Haber, D. A.; Toner, M. Microfluidic, marker free isolation of circulating tumor cells from blood samples. *Nat. Protoc.* **2014**, *9*, 694−710.
(47) Wang, S.; Liu, K.; Liu, J.; Yu, Z. T. F.; Xu, X.; Zhao, L.; Lee, T.; Lee, E. K.; Reiss, J.; Lee, Y. K.; Chung, L. W. K.; Huang, J.; Rettig, M.; Seligson, D.; Duraiswamy, K. N.; Shen, C. K. F.; Tseng, H. R. Highly Efficient Capture of Circulating Tumor Cells by Using Nano structured Silicon Substrates with Integrated Chaotic Micromixers. *Angew. Chem., Int. Ed.* **2011**, *50*, 3084−3088.
(48) Wang, C.; Ye, M.; Cheng, L.; Li, R.; Zhu, W.; Shi, Z.; Fan, C.; He, J.; Liu, J.; Liu, Z. Simultaneous isolation and detection of circulating tumor cells with a microfluidic silicon nanowire array integrated with magnetic upconversion nanoprobes. *Biomaterials* **2015**, *54*, 55−62.
(49) Brinkmann, F.; Hirtz, M.; Haller, A.; Gorges, T. M.; Vellekoop, M. J.; Riethdorf, S.; Müller, V.; Pantel, K.; Fuchs, H. A Versatile Microarray Platform for Capturing Rare Cells. *Sci. Rep.* **2015**, *5*, 15342.
(50) van Dongen, J. J. M.; van der Velden, V. H. J.; Bruggemann, M.; Orfao, A. Minimal residual disease diagnostics in acute lymphoblastic leukemia: need for sensitive, fast, and standardized technologies. *Blood* **2015**, *125*, 3996−4009.
(51) Borowitz, M. J.; Devidas, M.; Hunger, S. P.; Bowman, W. P.; Carroll, A. J.; Carroll, W. L.; Linda, S.; Martin, P. L.; Pullen, D. J.; Viswanatha, D.; Willman, C. L.; Winick, N.; Camitta, B. M. Clinical significance of minimal residual disease in childhood acute lymphoblastic leukemia and its relationship to other prognostic factors: a Children's Oncology Group study. *Blood* **2008**, *111*, 5477−5485.
(52) Wang, Y.; Zhang, M.; Feng, L.; Dong, B.; Xu, T.; Li, D.; Jiang, L.; Chi, L. Tape Imprinted Hierarchical Lotus Seedpod Like Arrays for Extraordinary Surface Enhanced Raman Spectroscopy. *Small* **2019**, *15*, 1804527.